Journal of Peptide Science
J. Pept. Sci. 2008; **14**: 731–741
Published online 5 February 2008 in Wiley InterScience (www.interscience.wiley.com). DOI: 10.1002/psc.990

JOURNAL OF PEPTIDE SCIENCE

Aggregation of Aβ(1–42) in the presence of short peptides: conformational studies

ILONA LACZKÓ,[a]* ELEMÉR VASS,[b] KATALIN SOÓS,[c] LIVIA FÜLÖP,[c] MÁRTA ZARÁNDI[c] and BOTOND PENKE[c]

[a] Institute of Biophysics, Biological Research Centre of the Hungarian Academy of Sciences, H-6701 Szeged, Hungary
[b] Department of Organic Chemistry, Eötvös Lóránd University, H-1117 Budapest, Hungary
[c] Department of Medicinal Chemistry and Protein Research Group of the Hungarian Academy of Sciences, University of Szeged, H-6720 Szeged, Hungary

Received 19 June 2007; *Revised 19 October 2007*; *Accepted 31 October 2007*

Abstract: CD and infrared spectroscopic studies were performed on (i) the inhibitory effects of equimolar quantities of LPFFD-OH and LPYFD-NH_2 on the time-dependent aggregation of amyloid β-protein (Aβ) (1–42) and (ii) the β-sheet-breaker effects of two-fold molar excess of the pentapeptides on aggregated Aβ(1–42) aged 1 week. The data obtained from the time-dependent studies demonstrated that LPFFD-OH did not significantly influence, whereas LPYFD-NH_2 exerted some inhibitory effect on the aggregation of Aβ(1–42). When added to a solution of Aβ(1–42) aged 1 week, LPFFD-OH accelerated, while LPYFD-NH_2 delayed, but did not prevent further fibrillogenesis. The difference in the effects of these two pentapeptides on the aggregational profile of Aβ(1–42) is probably due to the difference in their conformational preferences: LPFFD-OH adopts a β-turn and extended structures, while LPYFD-NH_2 adopts a prevailing β-turn conformation. Copyright © 2008 European Peptide Society and John Wiley & Sons, Ltd.

Keywords: Alzheimer's disease; β-amyloid; inhibitory pentapeptides; fibrillogenesis; circular dichroism; infrared spectroscopy

INTRODUCTION

One of the most characteristic pathological markers of Alzheimer's disease (AD) is the accumulation of extracellular insoluble amyloid deposits in the brain [1,2]. These deposits contain the amyloid β-protein (Aβ), which is a 39–43-residue amphipathic molecule formed during the enzymatic cleavage of the amyloid precursor protein. Aβ(1–40) is the most prevalent species; Aβ(1–42) is more toxic [3–5]. Experimental data strongly suggest that the conformation and aggregation state have a crucial effect on the mechanism of neurotoxicity of Aβ. Aβ(1–42) molecules form fibrillar structures composed mainly of cross-β sheets [6,7]. The X-ray data indicate that in the cross-β structure the β-strands are perpendicular to the fiber axis, with interstrand H-bonding parallel to the fiber axis [8]. The fibrillization of Aβ plays a central role in the pathogenesis of the disease: fibrillar Aβ induces neuritic dystrophy [9], neuronal apoptosis [10], activates microglia [11], causes axonopathy via hyperphosphorylation and dissociation of the microtubule-associated tau protein [5,12], and rapidly enhances *N*-methyl-D-aspartate (NMDA) receptor function, while ablating α-amino-3-hydroxy-5-methyl-4-isoxazole-propionic acid (AMPA) induced neuronal firing rate [13]. On the other hand, Aβ monomers are not associated with neuronal dysfunction, and Aβ plaques themselves do not cause memory impairment too, until they occupy a substantial portion of the tissue volume in cerebral cortex and hippocampus [14]. The consensus might be that the harmful Aβ species are larger than monomers but smaller than the nonmobile superaggregates in plaques, and both oligomeric and fibrillar Aβ aggregates are targets for drug design in AD research [15–17].

Short peptides and small molecules can influence the structure and aggregation of Aβ and prevent fibril formation; therefore these are effective neuroprotective agents [18–25]. These results prompted further investigations of different types of aggregates, the pathway of Aβ fibrillization under different conditions, the design of inhibitors, and the screening of known drugs as potential Aβ oligomerization/fibrillogenesis inhibitors.

Peptides – homologous to the central hydrophobic region of Aβ and exhibit a similar degree of hydrophobicity, but a low propensity to adopt a β-sheet conformation – bind to Aβ and inhibit amyloid formation *in vitro* and disaggregate preformed Aβ fibrils [21–25]. Soto *et al.* designed inhibitors where the 17–20 sequence (LVFF) of Aβ served as a template for the synthesis of β-sheet-breaker pentapeptides [21,22]. Val was replaced by Pro in order to decrease the β-sheet-forming ability, and a charged residue (Asp) was added to increase the solubility of the peptide. Incubation of Aβ(1–42) for 7 days with an equimolar amount or a 20-fold molar excess of the pentapeptide LPFFD resulted in 34 and 72% inhibition of the fibrillogenesis, respectively. This peptide also induced a disassembly of preformed amyloid fibrils *in vitro*.

*Correspondence to: Ilona Laczkó, Institute of Biophysics, Biological Research Centre of the Hungarian Academy of Sciences, H-6701 Szeged, Hungary; e-mail: laczko@nucleus.szbk.u-szeged.hu

We have synthetized an analog of Soto's pentapeptide, in which Phe3 is replaced by the more hydrophilic Tyr. The objective of our present study was to establish whether LPYFD-NH_2 shows an improved efficiency of inhibiting the fibrillogenesis or disrupting preformed fibrils of Aβ(1–42) compared to LPFFD-OH. The conformational changes accompanying the aggregation and fibril formation of Aβ(1–42) alone or in the presence of LPFFD-OH and LPYFD-NH_2 were followed by means of CD and FTIR spectroscopy.

MATERIALS AND METHODS

Peptide Synthesis

Aβ(1–42) was synthetized as reported earlier [26]. LPFFD-OH, LPYFD-NH_2, and GGGGG-NH_2 were synthetized in the solid phase by using Boc chemistry. The peptides were purified on a C-4 RP-HPLC column with an acetonitrile gradient; pure fractions were pooled and lyophilized. Purity control and proof of structure were performed by amino acid analysis and ESI MS (FinniganMat TSQ 7000). The Aβ(1–42) used for spectroscopic measurements was pretreated by dissolution in neat HFIP, left to stand at room temperature for 24 h and then lyophilized. After repeated dissolution in a 1 : 1 mixture of HFIP : water, the peptide was immediately relyophilized.

CD Spectroscopy

CD measurements were performed at 25 °C on a Jobin–Yvon Mark VI dichrograph using a quartz cell of 0.1-cm pathlength. All the spectra were the averages of four scans; the resolution was 0.2 nm. The Aβ(1–42) was dissolved in tridistilled water (pH ~ 6) at a concentration of 0.2 mg/ml (44 μM). CD spectra were expressed as mean residue ellipticity $[\Theta]_{MR}$ in units of deg cm^2 $dmol^{-1}$, using a mean residue weight of 110. In some cases, CD spectra are given in ΔA, which is the difference between the absorbance of left and right circularly polarized light. The samples were sonicated for 5 min immediately after dissolution in water and prior to aging. For aging, the samples were kept at room temperature in glass vials. Aliquots were withdrawn after given time intervals and returned to the glass vials after the spectra had been recorded. The inhibitory and control pentapeptides were treated in the same way as the Aβ(1–42). The percentages of secondary structures were calculated by the Provencher–Glöckner curve analyzing algorithm [27].

FTIR Spectroscopy

Transmission FTIR measurements were made on a Bruker Equinox 55 instrument equipped with a liquid N_2-cooled MCT detector. A CaF_2 cell with a 50-μm teflon spacer was used. The protein concentration was 2 mg/ml in D_2O. The peptides were present as TFA salts. To estimate the secondary structure, the amide I region of the spectra was decomposed into individual bands by means of the Levenberg–Marcquardt nonlinear curve-fitting method, using weighted sums of Lorentzian and Gaussian functions. The contribution of each component to the amide I band was evaluated by integrating the area under the curves and normalizing to the total area of the amide I band.

RESULTS

CD Studies

Two sets of experiments were carried out. (i) To investigate the inhibitory effects of the pentapeptides LPFFD-OH and LPYFD-NH_2 on the *time-dependent aggregation* of Aβ(1–42), it was colyophilized with the pentapeptides and aged for 1 week. The molar ratio (r_M) of the pentapeptides to Aβ(1–42) was 1 and 10. (ii) To *study the β-sheet-breaker* effects, two equivalents ($r_M = 2$) of the pentapeptides were added to Aβ(1–42) that had been aged for 1 week at room temperature, and the mixtures were further incubated for 1 week.

The pentaglycine $(Gly)_5$ used in the control experiments made no CD contribution at any concentration and did not influence the aggregation of Aβ(1–42) at any r_M value (data not shown).

Effect of pretreatment on the solubility of Aβ(1–42). Figure 1 depicts the CD spectrum of Aβ(1–42) measured immediately after dissolution in neat HFIP. The Provencher–Glöckner curve-analyzing algorithm yielded 18% α-helix, 57% β-sheet, and 26% unordered conformations. After the sample had been left at room temperature for 24 h, the spectrum reflected a considerable degree of conformational change: the α-helix and β-sheet contents had decreased to 9 and 46%, respectively, while the amount of the unordered conformation had increased to 45%. When an aliquot of the HFIP solution of the 24-h sample was diluted with water to give a water : HFIP ratio of 1 : 1 and measured immediately, the α-helix content increased markedly, to 36%, the β-sheet content increased only slightly, to 49%, and that of the unordered conformation decreased, to 15%. The use of this 1 : 1 solvent mixture was found to improve the solubility of Aβ(1–42) relative to that in neat HFIP. The better solubility may be a consequence of the more expressed α-helix-promoting effect of the 1 : 1 water : HFIP mixture compared to that of neat HFIP.

The CD spectra of LPFFD-OH and LPYFD-NH_2. To reveal the conformational changes in these two pentapeptides in the presence of Aβ(1–42), CD titration was performed by increasing the TFE content of their aqueous solutions (Figure 2). TFE is known to be a suitable solvent with which to mimic the conformations adopted by short flexible peptides in the membrane or in other hydrophobic environments (e.g. the protein interior) [28]. In water, the spectra of both pentapeptides exhibited a positive band (L_a), at 218 nm for LPFFD-OH and at 225 nm for LPYFD-NH_2, which is attributed to the aromatic chromophores of Phe and Tyr. In general, the interaction of the peptide backbone with

DOI: 10.1002/psc

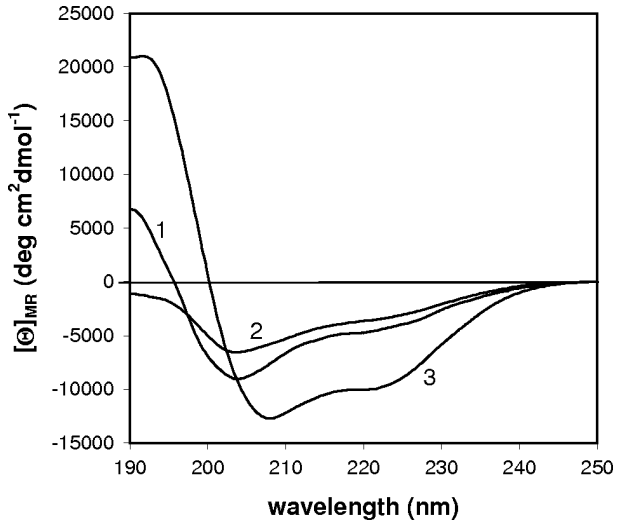

Figure 1 CD spectrum of Aβ(1–42) in neat HFIP measured at $t = 0$ (1) and after 24 h incubation at room temperature (2); after addition of water to the 24-h sample giving a water : HFIP ratio of 1 : 1 (v/v) (3). The concentration of the peptide was 68 μM and a cell with a pathlength of 0.05 cm was used.

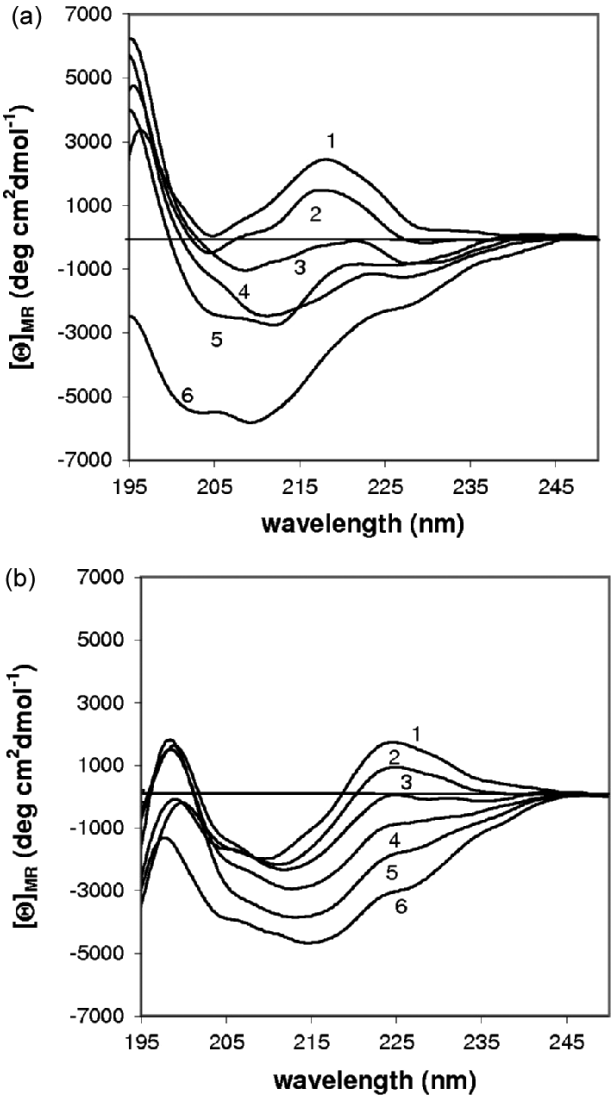

Figure 2 CD spectra of LPFFD-OH (a) and LPYFD-NH_2 (b) at different percentages of TFE in water. The concentration of the peptides was 0.3 mg/ml, and a cell with pathlength of 0.05 cm was used. (1) water (2) 10%; (3) 25%; (4) 50%; (5) 75% and (6) 100%.

the aromatic side-chain in a favorable conformation results in a positive L_a band, but less favorable conformations may give a negative L_a band [29]. On increase of the TFE content, the intensity of the L_a band decreased, while that of the broad negative band in the interval 195–220 nm gradually increased. It is interesting to note that the spectrum of LPYFD-NH_2 in water already contains a negative band, as an indication that the replacement of one of the Phe by Tyr decreases the flexibility of the peptide and induces a definite secondary structure even in water. In 100% TFE, the spectra of both peptides are dominated by an induced secondary structure, but the shapes of the spectra are different: for LPYFD-NH_2, the negative band is much broader than that for LPFFD-OH. This is due to the appearance of a negative shoulder at ~228 nm, which is more intense in the spectrum of LPYFD-NH_2 and can be explained by the positive → negative transition of the L_a band on passing from water to TFE. In an earlier study on the model dipeptide Ac-FY-NH_2 a similar spectral change was observed upon decrease of the polarity of the solvent [30]. The CD spectrum suggests that in TFE LPYFD-NH_2 adopts a prevailing β-turn conformation (which is already present in water), while LPFFD-OH is present as a mixture of turn and extended conformations. The reason for the difference in spectral behavior is that the β-turn-forming propensity (P_t) of Tyr is much higher (1.14) than that of Phe (0.6) [31], which has a stabilizing effect on the β-turn conformation in LPYFD-NH_2.

Time-dependent aggregation of Aβ (1–42). Figure 3(a) shows the CD spectrum of Aβ(1–42) alone in water as a function of the aging time. Lyophilization of the Aβ(1–42) in the 1 : 1 water : HFIP mixture resulted in a clear solution even in water at pH ~ 6. The broad negative band in the spectrum of Aβ(1–42) at $t = 0$ reflects a mixture of β-sheet and unordered conformers and is attributed mainly to the $n\pi^*$ transition (215 nm) of the β-sheet structure. The $\pi\pi^*$ transition of the β-sheet, which is expected to give a positive band below 200 nm, is suppressed by the strong negative band of the unordered conformation. As the peptide underwent aging, a gradual spectral change was observed: the intensity of the positive band increased, reaching its maximum at 48 h. This reflects a conformational transition from an unordered-rich form to a β-sheet-rich form. After aging for 120 or 168 h, the intensities of both the positive and the negative band were decreased and a red shift (215 → 226 nm) of the negative band

DOI: 10.1002/psc

could be seen. Similar red-shifted β-sheet spectra have been observed for a number of other peptides, and the shifts have been attributed to the appearance of distorted (helically twisted) β-strands [32–34].

Time-dependent aggregation of Aβ(1–42) in the presence of LPFFD-OH and LPYFD-NH$_2$. At $r_M = 1$, the spectral behavior of Aβ(1–42) in the presence of LPYFD-NH$_2$ is similar to that of Aβ(1–42) alone, i.e. this pentapeptide does not influence the aggregational profile significantly (Figure 3(b)). In the presence of LPFFD-OH, however, the higher intensity of the negative band at 226 nm after aging for 168 h indicates the presence of a somewhat higher amount of distorted β-sheets (Figure 3(c)). The CD contribution of the pentapeptides to the spectrum of Aβ(1–42) at $r_M = 1$ and 2 is not measurable because of their low concentrations [0.027 (44 μM) and 0.054 mg/ml (88 μM), respectively].

At $r_M = 10$, the CD spectra were taken between 205 and 250 nm (Figure 4(a)–(d)), because of the high absorbances (>1) of the pentapeptides below 205 nm (measured in a 1-mm cell). Since the pentapeptides give CD bands of significant intensity in the spectral region 205–250 nm, the measured spectra of the mixtures of Aβ(1–42) and the pentapeptides (curves 3) were compared with the calculated summed spectra (curves 4) of free Aβ(1–42) (curves 1) and the free pentapeptides (curves 2). Only minor differences were to be seen between the measured spectra of the mixtures and the summed spectra of the individual Aβ(1–42) and LPFFD-OH recorded at 0 h (Figure 4(a)) and after aging for 168 h (Figure 4(b)). However, considerable deviation of the summed spectrum from the measured one in the presence of LPYFD-NH$_2$ was observed after aging for 168 h. The measured spectrum of the mixture of Aβ(1–42) + LPYFD-NH$_2$ was a typical β-sheet spectrum both at 0 and at 168 h (Figure 4(c) and (d)). The difference between the summed and measured spectrum at 168 h may stem from the unordered $\rightarrow$ β-sheet conformational transition of Aβ(1–42), induced by LPYFD-NH$_2$ even at 0 h (Figure 4(c)), the induced β-sheet conformation being preserved throughout the 168-h incubation period (Figure 4(d)). Nevertheless, when the small peptides give measurable CD contributions in the observed spectral range like at $r_M = 10$, the results must be interpreted with caution. As the conformational changes in the pentapeptides in the presence of Aβ(1–42) are not known, the spectral changes of the mixtures may be due to changes in both Aβ(1–42) and the pentapeptides. This is confirmed by the results of the TFE titration experiments, which appear to indicate considerable conformational changes in the pentapeptides in association with Aβ(1–42) (Figure 2).

It is important that the pentapeptides alone in water did not demonstrate any significant spectral change during a 1-week incubation period, which suggests no aggregation.

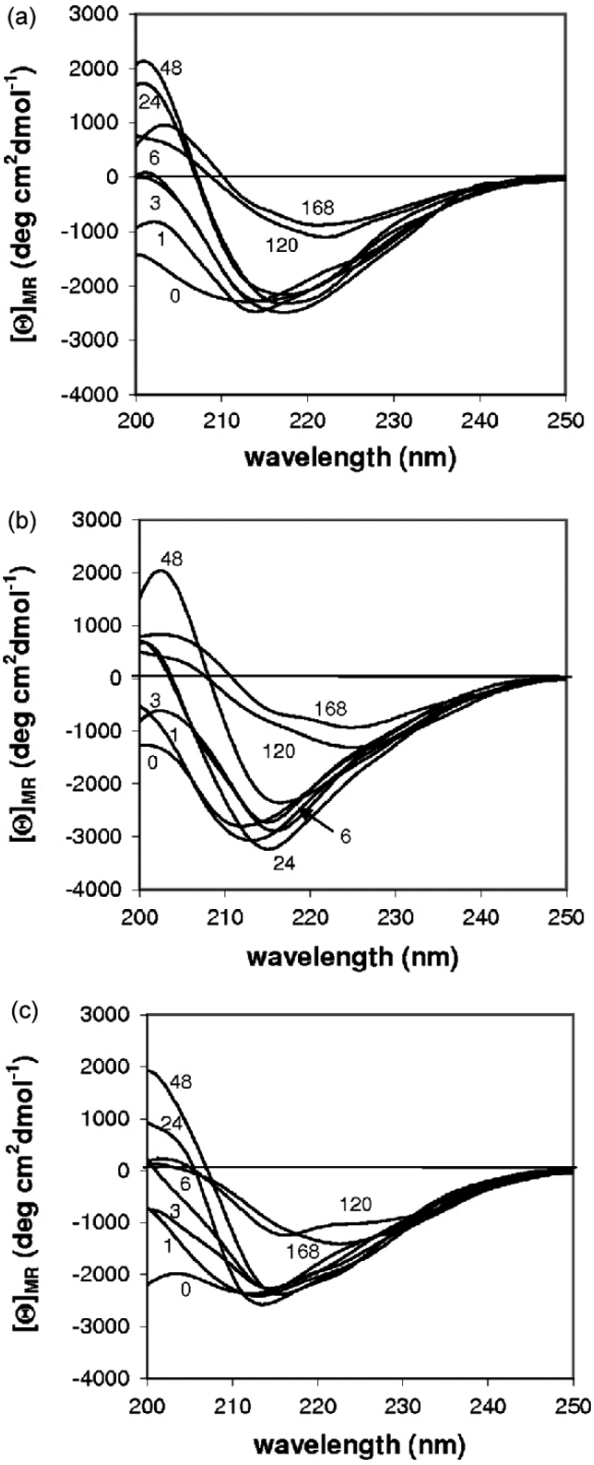

Figure 3 CD spectrum of Aβ(1–42) in water (pH ~ 6) aging alone and together with equimolar quantity ($r_M = 1$) of the pentapeptides for 168 h at room temperature. The concentration of Aβ(1–42) was 44 μM and a cell of 0.1 cm was used. The numbers on the curves denote the sampling time in hours. (a) Aβ(1–42) aging alone; (b) Aβ(1–42) + LPYFD-NH$_2$; (c) Aβ(1–42) + LPFFD-OH.

DOI: 10.1002/psc

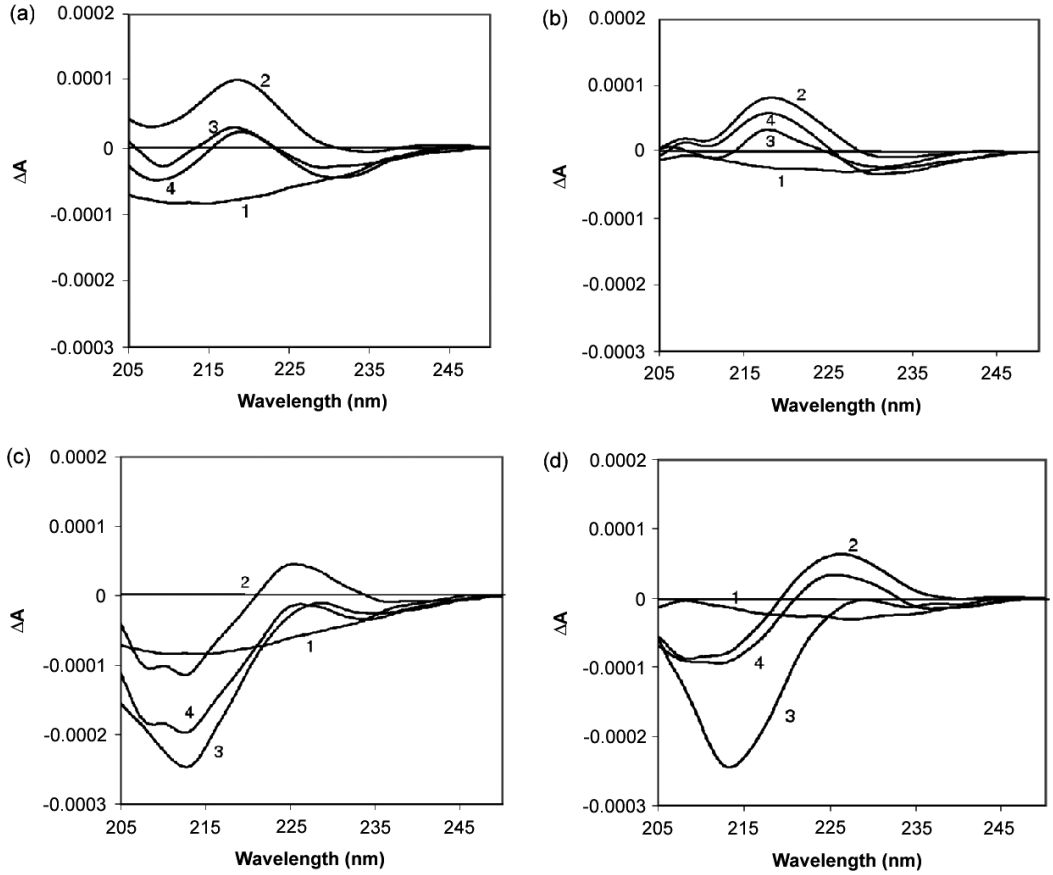

Figure 4 Effect of the pentapeptides on the CD spectrum of Aβ(1–42) aging together for 168 h at room temperature. The concentration of Aβ(1–42) was 44 μM in water (pH ~ 6) and the pentapeptides were present in ten-fold molar excess ($r_M = 10$). (a) Aβ(1–42) + LPFFD-OH at $t = 0$ h; (b) Aβ(1–42) + LPFFD-OH at $t = 168$ h; (c) Aβ(1–42) + LPYFD-NH_2 at $t = 0$ h; (d) Aβ(1–42) + LPYFD-NH_2 at $t = 168$ h. (1), Aβ(1–42) alone; (2), pentapeptide alone; (3), measured spectra of Aβ(1–42) + pentapeptide (4) summed spectra of Aβ(1–42) alone and pentapeptide alone.

***β*-Sheet-breaker effects of LPFFD-OH and LPYFD-NH_2.** Figure 5 illustrates the change in the CD spectrum of Aβ(1–42) alone in water, measured at 0, 1, and 2 weeks. There were noteworthy differences between the spectrum of the Aβ(1–42) solution which was incubated unperturbed for 1 week (Figure 5) and that of the solution which was disturbed by frequent sampling during 1 week (Figure 3(a)). This observation underlines the importance of experimental circumstances which can induce or accelerate aggregational events. The negative band in the spectrum gradually shifts to longer wavelengths during the 2-week incubation, with a concomitant decrease in intensity of the negative band and an increase in that of the positive band. The CD spectrum of Aβ(1–42) after aging for 1 week revealed some helical features: the amount of ordered conformational elements (β-sheet and possibly α-helix) was increased, and that of the unordered conformation was decreased. After 2 weeks, the red-shifted CD spectrum reflected the accumulation of twisted β-sheet (the negative band at ~226 nm). Following addition of the inhibitors ($r_M = 2$) to the solution of Aβ(1–42) aged for 1 week, considerable spectral

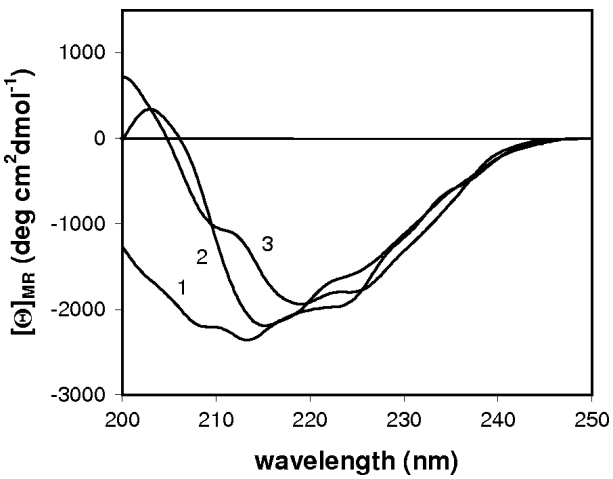

Figure 5 Change of the CD spectrum of Aβ(1–42) in a 2-week aging period. The concentration of Aβ(1–42) was 44 μM in water (pH ~ 6) and a cell with pathlength of 0.1 cm was used. (1) 0 h (2) 1 week (3) 2 weeks.

changes were observed [see the differences between the summed (curves 2) and measured spectra (curves 3) in Figure 6(a) and (b)]. However, the spectral responses

DOI: 10.1002/psc

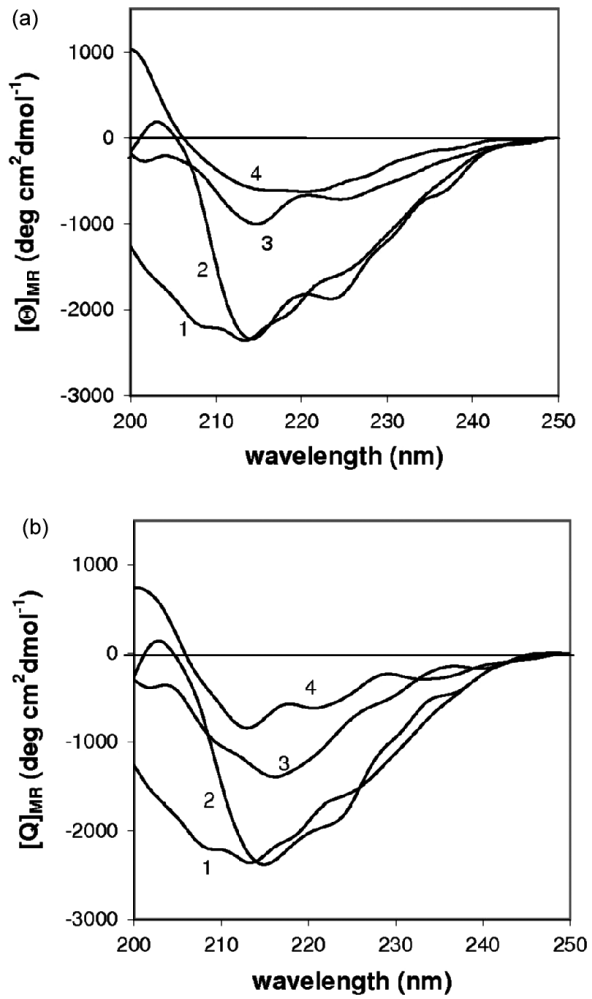

Figure 6 Effect of LPFFD-OH and LPYFD-NH_2 at $r_M = 2$ on the CD spectrum of Aβ(1–42) aged for 1 week in water (pH ~ 6) at room temperature. The concentration of Aβ(1–42) was 44 μM and a cell with pathlength of 0.1 cm was used (a) Aβ(1–42) + LPFFD-OH; (b) Aβ(1–42) + LPYFD-NH_2. (1), Aβ(1–42) at 0 h; (2), the summed spectra of the Aβ(1–42) aged for 1 week alone and the inhibitor alone; (3), spectra of Aβ(1–42) aged for 1 week and measured immediately after adding the pentapeptides; (4), Aβ(1–42) aged for additional 1 week in the presence of pentapeptides.

induced by the two pentapeptides differed. In the presence of LPFFD-OH, Aβ(1–42) was a mixture of the normal β-sheet and distorted β-sheet (curve 3 in Figure 6(a)), while in the presence of LPYFD-NH_2, the prevalent conformation was the normal β-sheet (curve 3 in Figure 6(b)). After incubation of the Aβ(1–42) solution for another week in the presence of LPFFD-OH, the Aβ(1–42) consisted mostly of twisted β-sheet (curve 4 in Figure 6(a)), which probably indicates the formation of longer filaments. In contrast, in the presence of LPYFD-NH_2, the Aβ(1–42) still contained a significant amount of the normal β-sheet conformation, indicating the stabilization of possibly shorter filaments (curve 4 in Figure 6(b)).

Table 1 Characteristic amide-I frequencies of Aβ(1–42) alone and in the presence of equimolar LPFFD-OH or LPYFD-NH_2 in D_2O measured at $t = 3$ h and after aging for 168 h

Peptide	Band frequency[a],cm^{-1}	Assignment
Aβ(1–42)		
$t = 3$ h	1628 (25)	β-sheet[d]
	1643 (11)	β-turn
	1656 (15)	Unordered/α-helix
	1673 (42)	[b]
	1691 (4)	[c]
$t = 168$ h	1624 (29)	β-sheet[d]
	1641 (13)	β-turn
	1655 (13)	Unordered/α-helix
	1673 (40)	[b]
	1691 (5)	[c]
Aβ(1–42) + LPYFD-NH_2		
$t = 3$ h	1626 (30)	β-sheet[d]
	1643 (12)	β-turn
	1656 (12)	Unordered/α-helix
	1673 (41)	[b]
	1689 (5)	[c]
$t = 168$ h	1624 (29)	β-sheet[d]
	1642 (13)	β-turn
	1656 (11)	Unordered/α-helix
	1673 (41)	[b]
	1689 (5)	[c]
Aβ(1–42)+LPFFD-OH		
$t = 3$ h	1625 (30)	β-sheet[d]
	1643 (12)	β-turn
	1656 (10)	Unordered/α-helix
	1673 (42)	[b]
	1692 (6)	[c]
$t = 168$ h	1624 (34)	β-sheet[d]
	1642 (12)	β-turn
	1655 (12)	Unordered/α-helix
	1673 (40)	[b]
	1689 (4)	[c]

[a] In parenthesis: relative intensities in percentages. Only component of ≥3% are listed.
[b] Contribution of COO^- of trifluoroacetate.
[c] High-frequency component band of antiparallel β-sheet.
[d] Intermolecular, twisted β-sheet.

FTIR Studies

The deconvoluted FTIR spectra of D_2O solutions of Aβ(1–42) alone and in the presence of equimolar LPFFD-OH or LPYFD-NH_2, measured after standing for 3 h and after aging for 1 week at room temperature, are shown in Figures 7–9. The samples were incubated for 3 h prior to scanning because of the H/D exchange. The peak positions and relative intensities of the component bands of the amide-I region (1600–1700 cm^{-1}) are listed in Table 1. The amide-I components are assigned to the secondary structures as follows: 1624–1628 cm^{-1}: the intermolecular

DOI: 10.1002/psc

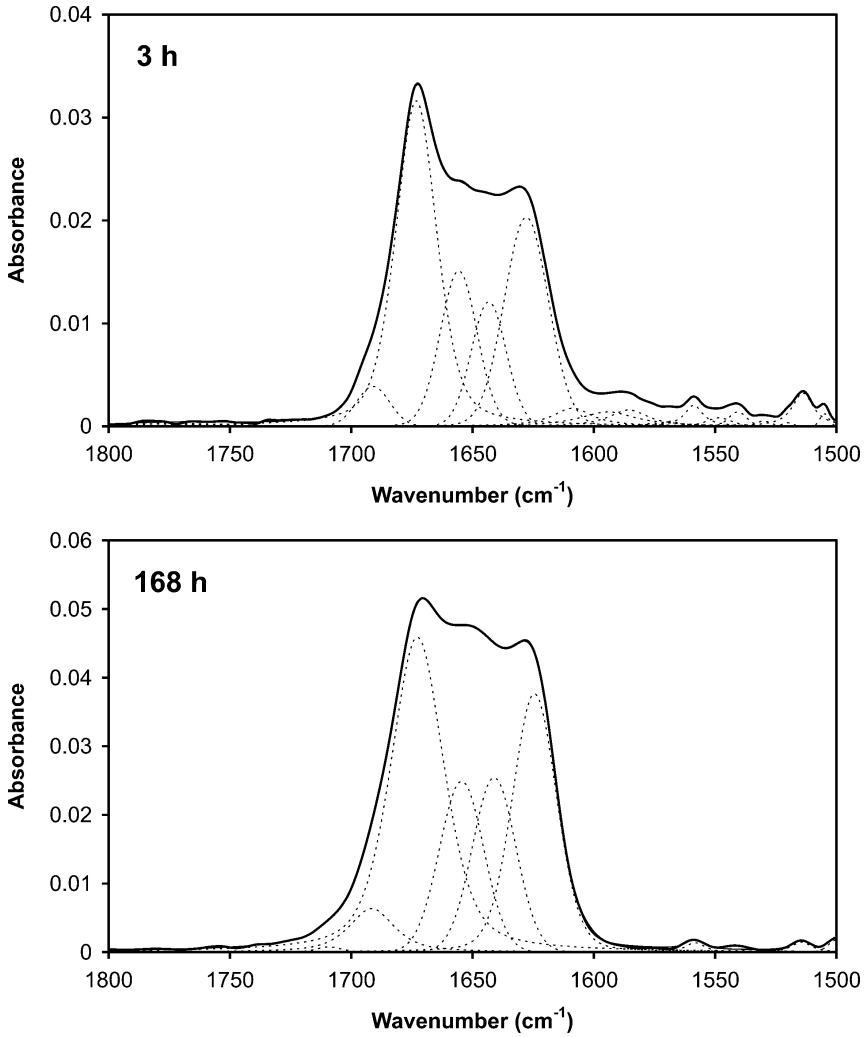

Figure 7 FTIR spectrum of Aβ(1–42) in D_2O measured after standing for 3 h and after aging for 168 h. The concentration of Aβ(1–42) was 2 mg/ml.

β-sheet/fibrils; the minor band at 1689–1692 cm^{-1}: the high-frequency contribution of the antiparallel β-sheet; 1641–1643 cm^{-1}: the H-bonded β-turn; 1655–1656 cm^{-1}: the unordered or α-helix conformation [35].

A previous investigation indicated that the native β-sheet proteins and the amyloid fibrils differ in the amide-I band: the native intramolecular β-sheet produces amide-I peaks between 1630 and 1640 cm^{-1}, while the range of amyloid fibrils extends from 1611 to 1630 cm^{-1} [36]. The amide-I maxima of β-sheet proteins correlate with the average number of strands per sheet and the twist angle: all native β-sheet proteins are characterized by a right-handed twist of the β-sheet [37]. *Ab initio* calculations have shown that the amide-I maximum is shifted to higher wavenumbers if the number of strands per β-sheet decreases, or if the twist angle is increased [38].

In all the samples investigated here, the position of the β-sheet band (1628–1624 cm^{-1}), together with the high-frequency antiparallel β-sheet component at around 1690 cm^{-1}, reflects the presence of the intermolecular H-bonded antiparallel β-sheet in the amyloid fibrils. The shift by a few wavenumbers after aging for 1 week is not of value since this falls within the 4 cm^{-1} resolution of the spectrophotometer. This means that already at $t = 3$ h, the Aβ(1–42) was present in fibrillar state because of the much higher Aβ(1–42) concentration applied in the FTIR measurements (2 mg/ml) relative to that in the CD studies (0.2 mg/ml).

Table 1 shows that the β-sheet content of Aβ(1–42) measured after standing for 3 h was 25%, which after aging alone for 1 week in D_2O had increased to 29%. The intensity of the β-sheet component band at 1626 cm^{-1} measured at $t = 3$ h was increased to 30% in the presence of either LPFFD-OH or LPYFD-NH_2. This value was not changed significantly when the Aβ(1–42) was aged with LPYFD-NH_2 for 168 h (30 → 29%), but it increased somewhat on aging with LPFFD-OH (30→ 34%).

DOI: 10.1002/psc

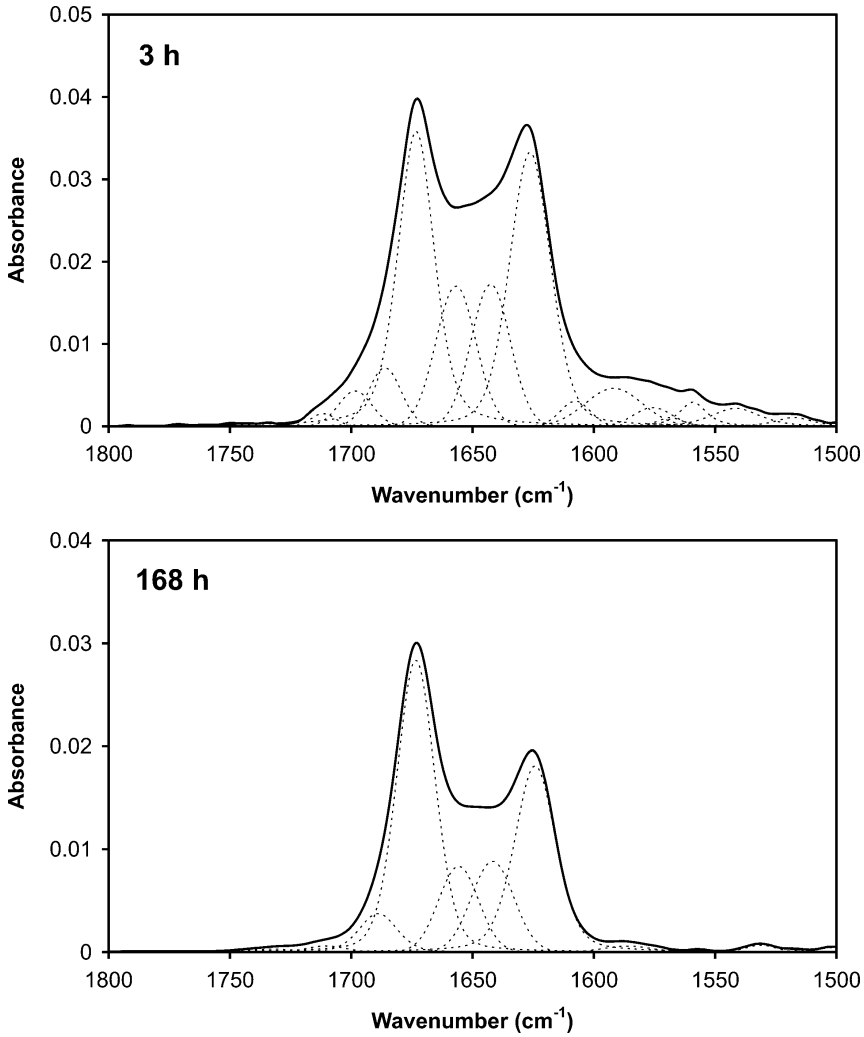

Figure 8 FTIR spectrum of Aβ(1–42) in D_2O in the presence of equimolar LPFFD-OH measured after standing for 3 h and after aging for 168 h. The concentration of Aβ(1–42) was 2 mg/ml.

DISCUSSION

This article reports CD and FTIR spectroscopic studies relating to the conformational changes during the aging of Aβ(1–42) in water alone or in the presence of pentapeptides, LPFFD-OH and LPYFD-NH_2. For these measurements, slightly acidic (pH$\sim$6) experimental conditions were used which promote aggregation and fibril formation [37,38]. Such a pH value is of physiological relevance, since the pH falls at sites of inflammation [39,40] and, accordingly, around inflammation-associated senile plaques.

Effects of LPFFD-OH and LPYFD-NH_2 on the Aggregation of Aβ(1–42) in the 168-h Incubation Period

The low-intensity red-shifted CD spectrum of Aβ(1–42) after aging for 168 h alone or in the presence of these short pentapeptides (Figure 3) may be due to the enrichment of twisted β-sheets in the aggregates of increasing size (filaments). Fasman classified polypeptides which give a 'normal' β-sheet CD spectrum as I-β, and those that give a red-shifted spectrum as II-β peptides [41]. Woody [29,34] suggested a structural basis for this distinction, noting that II-β polypeptides have a large fraction of residues in β-turns. This interpretation was supported by the fact that most II-β polypeptides form cross-β structures.

The CD spectral changes observed during the aging of Aβ(1–42) alone for 168 h suggested the gradual formation of slightly twisted II-β cross-β structures. This was confirmed by FTIR studies: the intensity of the component band at 1626 cm^{-1}, corresponding to the intermolecular or twisted β-sheet, increased from 25 to 29% (Table 1). In the presence of equimolar LPYFD-NH_2, the CD spectral analysis demonstrated that the formation of the cross-β structure was not influenced significantly, while a small effect was observed for LPFFD-OH. In the latter case, the slight increase in the intensity of the red-shifted negative band at

DOI: 10.1002/psc

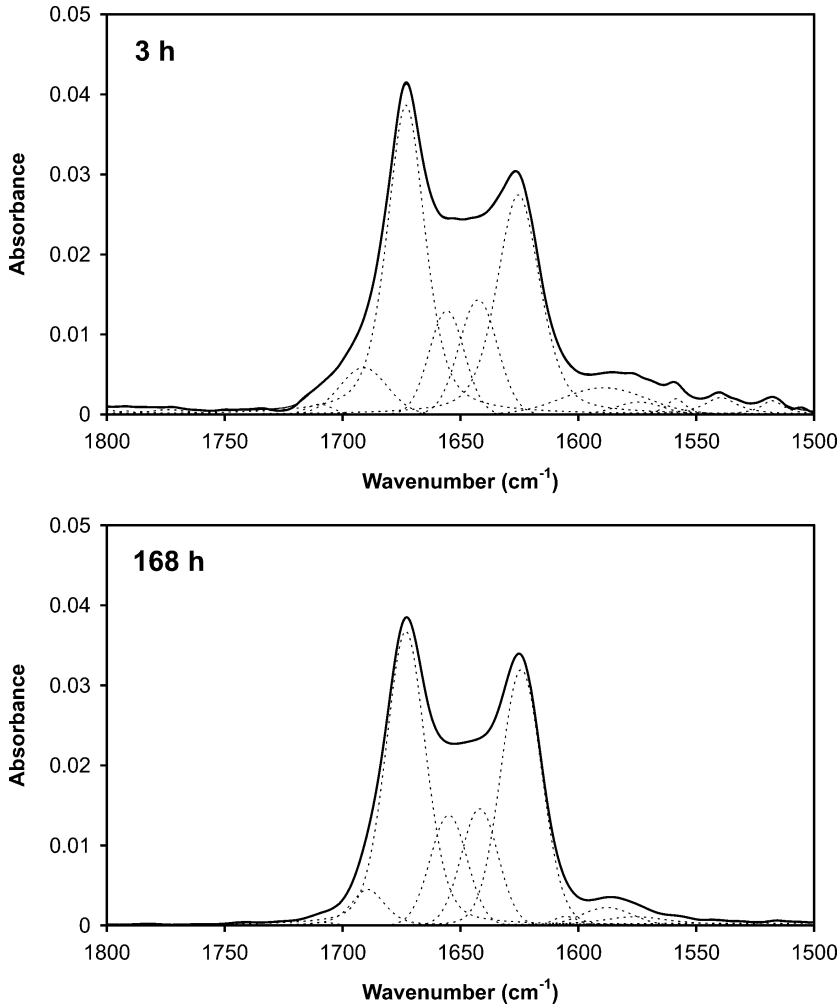

Figure 9 FTIR spectrum of Aβ(1–42) in D_2O in the presence of equimolar LPYFD-NH_2 measured after standing for 3 h and after aging for 168 h. The concentration of Aβ(1–42) was 2 mg/ml.

226 nm reflects a somewhat higher amount of slightly twisted cross-β sheet. The FTIR measurements also confirmed an increase in the amount of intermolecular cross-β sheet when Aβ(1–42) was aged together with LPFFD-OH; this increase was about the same (30–34%) as in the case of Aβ(1–42) aged alone. In the presence of LPYFD-NH_2, the amount of β-sheet practically did not change according to FTIR. All these data reveal that the time-dependent increase of cross-β structure of Aβ(1–42) was not prevented by LPFFD-OH, whereas LPYFD-NH_2 exerted some inhibitory effect.

Effects of LPFFD-OH and LPYFD-NH_2 on the Preformed Aβ(1–42) Assemblies

Addition of the pentapeptides at $r_M = 2$ to the Aβ(1–42) solution aged for 1 week caused a prompt, considerable, but different conformational change.

The conformational transition during the aging of Aβ(1–42) alone for 2 weeks is as follows:

state 1 — 1 week → state 2

unordered and normal β-sheet ⟶ unordered ↓ normal β-sheet ↑ twisted β-sheet ↑

1 week → state 3

⟶ normal β-sheet ↓ twisted β-sheet ↑

The CD analysis suggests that different aggregational profiles are plausible when LPFFD-OH or LPYFD-NH_2 is added to the Aβ(1–42) in state 2 and the mixture is aged for an additional 1 week:

DOI: 10.1002/psc

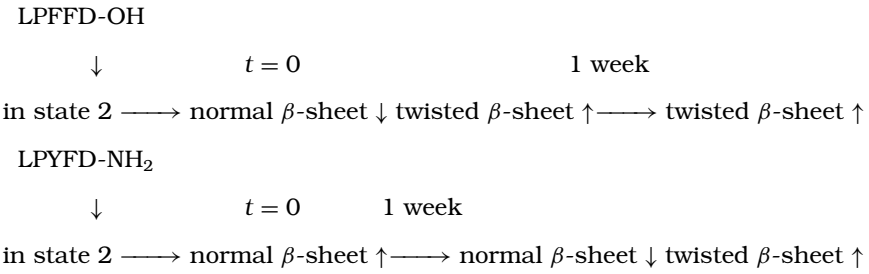

From the shape and intensity of the CD spectrum of Aβ(1–42) after prolonged incubation with LPFFD-OH (Figure 6(a)), the formation of helically twisted fibrils is highly probable. A similarly shaped CD spectrum was found by Kirkitadze *et al.* [37] when Aβ(1–40) was aged for 21 days. Concomitant electromicroscopic analysis of their sample revealed the formation of helically twisted fibrils. The CD spectrum of Aβ(1–42) aged for 1 week with LPYFD-NH_2, however, still indicated the presence of a significant amount of the normal β-sheet.

In brief, whereas LPFFD-OH accelerated, LPYFD-NH_2 was able to delay, but not prevent or reverse the conformational events leading to a further fibrillization of Aβ(1–42) aged for 1 week.

The difference in the effects of LPFFD-OH and LPYFD-NH_2 on the aggregation profile of Aβ(1–42) can be explained by the different conformational preferences of the two pentapeptides in a hydrophobic environment. In neat TFE [and probably when associated with Aβ(1–42)], LPFFD-OH is present as a mixture of β-turn and extended conformation, but LPYFD-NH_2 adopts a prevailing β-turn conformation. The conformation adopted by LPFFD-OH when it interacts with Aβ(1–42) may be favorable for the formation of an intermolecular H-bonded β-sheet of the amyloid molecules, while the turn conformation of LPYFD-NH_2 is not favored as concerns induction of the intermolecular β-sheet. Our studies emphasize the importance of the conformational preferences of the designed short peptides in exerting significant inhibitory effect on fibrillogenesis.

Acknowledgements

This work was supported by grants NKTH RET 108/2004 and OTKA T047186 and GVOP-3.2.1-2004-04-0345/3,0 for E.V.

REFERENCES

1. Clippingdale AB, Wade JD, Barrow CJ. The amyloid-beta peptide and its role in Alzheimer's disease. *J. Pept. Sci.* 2001; **7**: 227–249.
2. Lansbury PT, Lashuel HA. A century-old debate on protein aggregation and neurodegeneration enters the clinic. *Nature* 2006; **443**: 774–779.
3. Bayer TA, Wirths O, Majtényi K, Hartmann T, Multhaup G, Beyreuther K, Czech C. Key factors in Alzheimer's disease: beta-amyloid precursor protein processing, metabolism and intraneuronal transport. *Brain Pathol.* 2001; **11**: 1–11.
4. Dahlgren KN, Manelli AM, Stine WB, Baker LK, Krafft GA, LaDu MJ. Oligomeric and fibrillar species of amyloid-beta peptides differentially affect neuronal viability. *J. Biol. Chem.* 2002; **277**: 32046–32053.
5. Datki Z, Papp R, Zádori D, Soós K, Fülöp L, Juhász A, Laskay G, Hetényi C, Mihalik E, Zarándi M, Penke B. *In vitro* model of neurotoxicity of A beta 1-42 and neuroprotection by a pentapeptide: irreversible events during the first hour. *Neurobiol. Dis.* 2004; **17**: 507–515.
6. Serpell LC. Alzheimer's amyloid fibrils: structure and assembly. *Biochim. Biophys. Acta* 2000; **1502**: 16–30.
7. Petkova AT, Ishii Y, Balbach JJ, Antzutkin ON, Leapman RD, Delaglio F, Tycko R. A structural model for Alzheimer's β-amyloid fibrils based on experimental constraints from solid state NMR. *Proc. Natl. Acad. Sci. U.S.A.* 2002; **99**: 16742–16747.
8. Rochet JC, Lansbury PT Jr. Amyloid fibrillogenesis: themes and variations. *Curr. Opin. Struct. Biol.* 2000; **10**: 60–68.
9. Deshpande A, Mina E, Glabe C, Busciglio J. Different conformations of amyloid beta induce neurotoxicity by distinct mechanisms in human cortical neurons. *J. Neurosci.* 2006; **26**: 6011–6018.
10. Isaacs AM, Senn DB, Yuan ML, Shine JP, Yankner BA. Acceleration of amyloid beta-peptide aggregation by physiological concentrations of calcium. *J. Biol. Chem.* 2006; **281**: 27916–27923.
11. Butovsky O, Talpalar AE, Ben-Yaakov K, Schwartz M. Activation of microglia by aggregated beta-amyloid or lipopolysaccharide impairs MHC-II expression and renders them cytotoxic whereas IFN-gamma and IL-4 render them protective. *Mol. Cell. Neurosci.* 2005; **29**: 381–393.
12. Rapoport M, Dawson HN, Binder LI, Vitek MP, Ferreira A. Tau is essential to beta-amyloid-induced neurotoxicity. *Proc. Natl. Acad. Sci. U.S.A.* 2002; **99**: 6364–6369.
13. Szegedi V, Juhász G, Budai D, Penke B. Divergent effects of A beta 1-42 on ionotropic glutamate receptor-mediated responses in CA1 neurons in vivo. *Brain Res.* 2005; **1062**: 120–126.
14. Chen GQ, Chen KS, Knox J, Inglis J, Bernard A, Martin SJ, Justice A, McConlogue L, Games D, Freedman SB, Morris RGM. A learning deficit related to age and beta-amyloid plaques in a mouse model of Alzheimer's disease. *Nature* 2000; **408**: 975–979.
15. Oda T, Wals P, Osterburg HH, Johnson SA, Pasinetti GM, Morgan TE. Clusterin alters the aggregation of amyloid beta-peptide and forms slowly sedimentic A-beta complexes that cause oxidative stress. *Exp. Neurol.* 1995; **136**: 22–31.
16. Lambert MP, Barlow AK, Chromy BA, Edwards C, Reed R, Liosatos M. Diffusible, nonfibrillar ligands derived from Abeta(1-42) are potent central nervous system neurotoxins. *Proc. Natl. Acad. Sci. U.S.A.* 1998; **95**: 6448–6453.
17. Walsh DM, Hartley DM, Kusumoto Y, Fezoui Y, Vasquez S, Vassilev PM. Amyloid beta-protein fibrillogenesis–structure and

biological activity of protofibrillar intermediates. *J. Biol. Chem.* 1999; **274**: 25945–25952.
18. Cohen FE, Kelly JV. Therapeutic approaches to protein-misfolding diseases. *Nature* 2003; **426**: 905–909.
19. Talaga P. Inhibitors of beta-amyloid aggregation: still an issue of structure and function? *Drug Discov. Today: Therapeutic Strategies* 2004; **1**: 7–12.
20. Bieler S, Soto C. Beta-sheet breakers for Alzheimer's disease therapy. *Curr. Drug Targets* 2004; **5**: 553–558.
21. Soto C, Sigurdsson EM, Morelli L, Kumar RA, Castano EM, Frangione B. Beta-sheet breaker peptides inhibit fibrillogenesis in a rat brain model of amyloidosis: Implications for Alzheimer's therapy. *Nat. Med.* 1998; **4**: 822–826.
22. Soto C, Kindy MS, Baumann M, Frangione B. Inhibition of Alzheimer's amyloidosis by peptides that prevent beta-sheet conformation. *Biochem. Biophys. Res. Commun.* 1996; **226**: 672–680.
23. Sato T, Kienlen-Campard P, Ahmed M, Liu W, Li HL, Elliott JI, Aimoto S, Constantinescu SN, Octave JN, Smith SO. Inhibitors of amyloid toxicity based on beta-sheet packing of A beta 40 and A beta 42. *Biochemistry* 2006; **45**: 5503–5516.
24. Adessi C, Soto C. Beta-sheet breaker strategy for the treatment of Alzheimer's disease. *Drug Dev. Res.* 2002; **56**: 184–193.
25. Sato C, Castano EM, Kumar RA, Beavis RC, Frangione B. Fibrillogenesis of synthetic amyloid-beta peptides is dependent on their initial secondary structure. *Neurosci. Lett.* 1995; **200**: 105–108.
26. Zarándi M, Soós K, Fülöp L, Bozsó Z, Datki Z, Tóth GK, Penke B. Synthesis of Abeta(1-42) and its derivatives with improved efficiency. *J. Pept. Sci.* 2007; **13**: 94–99.
27. Provencher W, Glöckner J. Estimation of globular protein secondary structure from circular dichroism. *Biochemistry* 1981; **20**: 33–37.
28. Jackson M, Mantsch HH. Halogenated alcohols as solvents for proteins: FTIR spectroscopic studies. *Biochim. Biophys. Acta* 1992; **1118**: 139–143.
29. Woody RW. Circular dichroism of peptides. In *The Peptides*, Vol. 7, Udenfriend S, Meienhofer J, Hruby VJ (eds). Academic Press: New York, 1985; 15–113.
30. Laczkó I, Hollósi M, Ürge L, Ugen KE, Weiner DB, Mantsch HH, Thurin J, Ötvös L Jr. Synthesis and conformational studies of N-glycosylated analogues of the HIV-1 principal neutralizing determinant. *Biochemistry* 1992; **31**: 4282–4288.
31. Chou PY, Fasman GD. Empirical predictions of protein conformation. *Annu. Rev. Biochem.* 1978; **47**: 251–276.
32. Gordon DJ, Sciarretta K, Meredith SC. Inhibition of beta-amyloid(40) fibrillogenesis and disassembly of beta-amyloid congeners containing N-methyl amino acids at alternate residues. *Biochemistry* 2001; **40**: 8237–8245.
33. Zhang S, Rich A. Direct conversion of an oligopeptide from a beta-sheet to an alpha-helix: a model for amyloid formation. *Proc. Natl. Acad. Sci U.S.A.* 1997; **94**: 23–28.
34. Manning MC, Illangasekare M, Woody RW. Circular dichroism studies of distorted alpha-helices, twisted beta-sheets and beta-turns. *Biophys. Chem.* 1988; **31**: 77–86.
35. Surewicz KW, Mantsch HH. New insight into protein secondary structure from resolution-enhanced infrared spectra. *Biochim. Biophys. Acta* 1988; **952**: 115–130.
36. Zandomeneghi G, Krebs MRH, McCammon MG, Fandrich M. FTIR reveals structural differences between native beta-sheet and amyloid fibrils. *Protein Sci.* 2006; **13**: 3314–3321.
37. Fraser PE, Nguyen JT, Surewicz WK, Kirschner DA. pH-Dependent structural transitions of Alzheimer amyloid peptides. *Biophys. J.* 1991; **60**: 1190–1201.
38. Kirkitadze MD, Condron MM, Teplow DB. Identification and characterization of key kinetic intermediates in amyloid beta-protein fibrillogenesis. *J. Mol. Biol.* 2001; **312**: 1103–1119.
39. Atwood CS, Moir RD, Huang X, Scarpa RC, Bacarra NM, Romano DM, Tanzi RE, Bush AI. Dramatic aggregation of Alzheimer A beta by Cu(II) is induced by conditions representing physiological acidosis. *J. Biol. Chem.* 1998; **273**: 12817–12826.
40. Potempa LA, Kubak BM, Gewurz HJ. Effect of divalent metal-ions and pH upon the binding reactivity of human-serum amyloid P-component, a C-reactive protein homolog, for zymosan-preferential reactivity in the presence of copper and acidic pH. *J. Biol. Chem.* 1985; **260**: 2142–2147.
41. Greenfield N, Fasman GD. Computed circular dichroism spectra for the evaluation of protein conformation. *Biochemistry* 1969; **8**: 4108–4116.

DOI: 10.1002/psc